NEUROSCIENCE

Head direction cells in a migratory bird prefer north

Susumu Takahashi[1]*, Takumi Hombe[2], Sakiko Matsumoto[2], Kaoru Ide[1], Ken Yoda[2]*

Animals exhibit remarkable navigation abilities as if they have an internal compass. Head direction (HD) cells encoding the animal's heading azimuth are found in the brain of several animal species; the HD cell signals are dependent on the vestibular nuclei, where magnetic responsive cells are present in birds. However, it is difficult to determine whether HD cell signals drive the compass orientation in animals, as they do not necessarily rely on the magnetic compass under all circumstances. Recording of HD cell activities from the medial pallium of shearwater chicks (*Calonectris leucomelas*) just before their first migration, during which they strongly rely on compass orientation, revealed that shearwater HD cells prefer a north orientation. The preference remained stable regardless of geolocations and environmental cues, suggesting the existence of a magnetic compass regulated by internally generated HD signals. Our findings provide insight into the integration of the direction and magnetoreception senses.

INTRODUCTION

Animals exhibit remarkable navigation abilities. They tend to align their bodies along or perpendicular to magnetic field lines; this phenomenon, referred to as magnetic alignment, has been reported in several animals, including insects, amphibians, fish, birds, and mammals (*1*). During long-distance migration, migratory birds are capable of pinpointing the exact wintering grounds situated thousands of kilometers away from breeding grounds (*2*, *3*) and have magnetically sensitive proteins in their retina (*4*–*6*). However, the physiological basis of magnetic orientation and navigation in animals remains elusive (*7*).

Several studies have reported that head direction (HD) cells are found in the brains of various animals ranging from insects to fish and mammals; these cells increase their firing rates while the animal's head points in a particular azimuth regardless of the animal's position (*8*–*11*) and are considered the neural underpinning of a sense of direction. It is thought that the vestibular brainstem contributes to generating HD signals (*12*, *13*). Moreover, HD cells were recently reported in the medial pallium (MP) of birds (*14*), showing homology with the mammalian hippocampal formation (HPF) or parahippocampal region (PHR) (*15*). The mammalian HPF and PHR are neuronal substrates for spatial navigation because of the presence of space-responsive cells forming cognitive maps (*16*), including HD cells (*10*), place cells (*17*), grid cells (*18*), and their equivalents.

HD cells are not considered as a magnetic compass because these cells depend on self-motion cues with no clear relationship between their signals and compass orientation. However, several brain regions were shown to be activated by magnetic stimulation (*19*); magnetoreception in the brain of birds has been identified using an immediate early gene as a marker of neural activation in the vestibular brainstem, HPF, PHR, and thalamus (*20*, *21*). Furthermore, magnetic field–responsive (MR) cells have been found in the avian vestibular brainstem (*22*), overlapping anatomically with a locus of HD coding. This suggests that the HD and magnetoreceptive networks are integrated. However, as animals do not necessarily rely on the magnetic compass during spatial navigation (*23*), particularly in a cue-rich environment (*24*), it is currently unknown whether some HD cells are sensitive to magnetic direction.

Long-distance migratory birds navigate thousands of kilometers, although juveniles and adults often take different routes during global migration (*2*, *3*, *25*). For instance, we previously found that the compass orientation drives the streaked shearwater (*Calonectris leucomelas*) juveniles' direct routes to their destination regardless of risky mountain crossings, whereas adults avoid mountain ranges and exploit energy-efficient detours along the coastline (*26*, *27*). These age- and experience-dependent path differences suggest that juveniles (first-time migrants) heavily rely on the compass orientation. Therefore, both a sense of direction and compass orientation are critical at the onset of the migration of juvenile birds.

On the basis of neurophysiological evidence regarding the presence of HD and MR cells (*8*–*11*, *14*, *22*, *28*) and ecological evidence obtained from migratory birds (*2*, *3*, *7*, *25*–*27*, *29*), we hypothesized that the MP serves as an integration substrate for the sense of direction and magnetoreception, as well as the presence of compass-like neurons in juveniles. To test this hypothesis, we used tetrodes to conduct electrophysiological recordings of multiple single-neuronal activities from the MP of a long-distance migratory seabird, the streaked shearwater.

RESULTS

Using a lightweight logger capable of wirelessly recording neural activity from the brain of freely behaving wild animals (*30*), we recorded neural activities in the brain of 10 wild streaked shearwater chicks before their first migration flight (Fig. 1, A and B; table S1; and figs. S1 to S4). All recordings were performed while the shearwaters were voluntarily walking in a square (120 cm by 120 cm) or circular (80 or 120 cm in diameter) open arena with a high wall in a room or outside near the burrows. Histological verification revealed that most recording sites (15 of 16) were distributed at the apical or lateral regions (figs. S1, S3, and S4), and the remaining recording site was accidentally located off-target at the apical hyperpallium on the border between the dorsal pallium and MP. Therefore, we only analyzed 15 recording sessions from the MP of nine chicks in the following analyses.

HD cells in shearwater chicks

To detect the presence of HD cells in the MP with increased firing rates when the animal's head pointed in a specific azimuth direction,

[1]Laboratory of Cognitive and Behavioral Neuroscience, Graduate School of Brain Science, Doshisha University, Kyotanabe City, Kyoto 610-0394, Japan. [2]Graduate School of Environmental Studies, Nagoya University, Furo-cho, Chikusa-ku, Nagoya, Aichi 464-8601, Japan.
*Corresponding author. Email: stakahas@mail.doshisha.ac.jp (S.T.); yoda.ken@nagoya-u.jp (K.Y.)

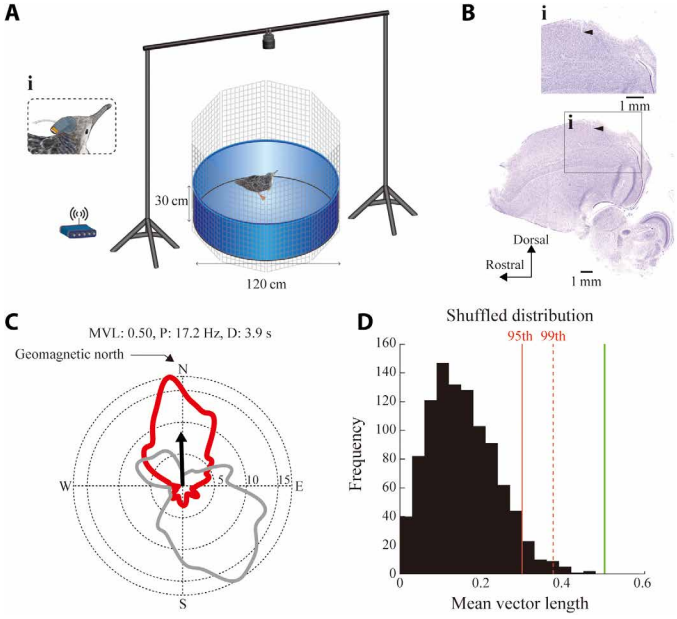

Fig. 1. HD cell in the MP of streaked shearwater chicks. (**A**) Multiple single-unit neural activities were wirelessly recorded from the MP of streaked shearwater chicks walking in an open arena using a lightweight logger (A, i). Neural activity was synchronized with the video camera mounted above the arena via a radio link transceiver (bottom left). (**B**) An electrode track in the Nissl-stained sagittal section of a chick's brain (3.72 mm lateral from midline). An arrowhead depicts the final location of the electrode tip. (B, i) Magnified image of the MP. Scale bars, 1 mm. (**C**) Polar plot of HD tuning curve of a representative HD cell (red) and behavioral HD (gray). Black vector originating from the center depicts the mean vector with a circular mean direction (CMD) and mean vector length (MVL) as a direction and magnitude, respectively. P, peak firing rate in hertz; D, dwell time in seconds. N, E, S, and W indicate geomagnetic north, east, south, and west, respectively. (**D**) Distribution of the MVL of shuffled data for the cell in (C). Red, red dotted, and green vertical lines depict the 95th and 99th percentiles of the shuffled distribution and the MVL of the cell in (C), respectively.

we calculated the mean vector length (MVL) of HD tuning. Of 95 cells recorded from nine shearwater chicks, 22 cells (~23%) met the criterion that the MVL exceeded the 95th percentile of the distribution of MVL calculated from shuffled data for each cell (Fig. 1, C and D). The number of HD cells was significantly larger than that expected by random selection from the distribution ($P < 0.00001$, one-tailed exact binomial test with an expected P_0 of 0.05, $n = 9$ chicks). The mean width of the HD tuning curve at the base (calculated at 50% peak rate) for the population of significant HD cells was 55° ± 35° (mean ± SD), mean modulation depth (peak to trough ratio) was 0.92, and MVL ranged from 0.14 to 0.67 (fig. S5), suggesting that HD tuning varies from broad to sharp. Furthermore, lateralization of the HD cells was not observed between the right and left cerebral hemispheres (right, 10 of 41 HD cells; left, 12 of 54 HD cells; Fisher's exact test, $P > 0.05$). HD cells were present in six of nine shearwater chicks, and the proportions were not significantly different (χ^2 test, $P > 0.05$; fig. S6). These results suggest the presence of HD cells in the MP of shearwater chicks.

Role of geolocation in HD cell orientation

Evidence on HD cells in the brain of mammals (*10*), fish (*8*), insects (*9*), and birds (*14*) suggests that the preferred directions of HD cells cover all directions and are uniformly distributed. As shown in Fig. 2A, HD cell firings pooled across all chicks covered nearly the entire range of 360°. However, the preferred directions were significantly confined to the north despite the lack of consistent and salient visual cues among experiments, including the arena orientation [circular mean direction (CMD) of 7° with geomagnetic north as a reference and MVL of 0.66; Rayleigh's test, $P < 0.0001$; Fig. 2, B and C, and fig. S7]. Moreover, a northward overrepresentation was inferred from single animals (fig. S8).

The preferred directions of the identified HD cells between the first and second halves of the session were significantly correlated (Pearson correlation $r = 0.64$, $P < 0.01$; Fig. 3A). Moreover, the preferred directions split by the median walking speed (Pearson correlation $r = 0.82$, $P < 0.00001$; Fig. 3B), between the west and east halves (Pearson correlation $r = 0.59$, $P < 0.01$), and between the north and south halves (Pearson correlation $r = 0.52$, $P < 0.05$) of the arena were significantly correlated (Fig. 3, C and D). In contrast, we calculated the within-session correlation of the HD tuning curve between the bisected data with respect to space, time, and walking speed. The preferred direction of HD cells with a significant within-session correlation (Pearson correlation, $P < 0.01$) was generally confined to the north (CMD of 3° to 23; fig. S9). These results suggest that the preferred direction of HD cells in the MP of shearwater chicks remained stable over space, time, and walking speed.

The geolocation and distal sensory cues differed between the indoor (conducted in a room ~2.5 km away from the burrows) and outdoor (conducted ~1.0 km away from the burrows) experiments (see Materials and Methods). However, the preferred directions for the population of HD cells in the indoor and outdoor experiments remained north and did not significantly differ (indoor experiment: CMD of 16° and MVL of 0.67; Rayleigh's test, $P < 0.001$; outdoor experiment: CMD of 347° and MVL of 0.71; Rayleigh's test, $P < 0.05$; Watson-Williams test, $P > 0.22$; Fig. 3, E and F). To estimate the preference of the behavioral heading direction, we calculated the dwell time, i.e., the amount of time when the chicks faced each HD. In contrast, the preferred directions of the dwell time in the behavioral HD pooled over the indoor and outdoor experiments did not deviate significantly from a random distribution, respectively (indoor experiment: CMD of 154° and MVL of 0.44; Rayleigh's test, $P > 0.44$; outdoor experiment: CMD of 194° and MVL of 0.12; Rayleigh's test, $P > 0.87$; fig. S10). However, as demonstrated in Figs. 1 and 2, the behavioral heading direction for individual animals exhibited a slightly inhomogeneous distribution. This may have biased the HD tuning curves. To address this concern, we subsampled the behavioral distribution to obtain equal numbers of samples in each directional bin and then computed subsampled neural tuning curves for the HD cells. The overall mean CMD of the equally subsampled HD tuning curves was used as a preferred direction of the HD cell. As a result, the preferred direction pooled across all HD cells remained as north (CMD of 2° and MVL of 0.66; Rayleigh's test, $P < 0.0001$; fig. S11).

Even when we performed recordings in the same shearwater chick, the recording locations in each session of experiments were more than 0.2 mm apart because the electrodes were moved between sessions using independently movable microdrives. Therefore, we assumed that multiple recording sessions from the same shearwater chick never repeatedly sampled the same cells and were pooled across all sessions. However, we could not reject the possibility that some cells were double counted. To address this concern, we further evaluated all possible combinations of HD cells collected only once

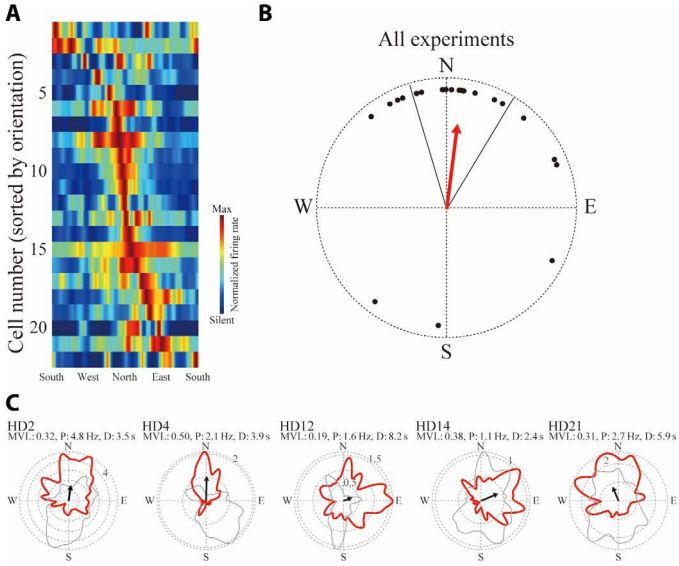

Fig. 2. HD cells prefer to align north. (**A**) Firing map showing each directional tuning curve of 22 significant HD cells normalized by each peak rate as a function of cardinal direction. The cell order was sorted by the orientation of the peak rate. The map is color coded according to the scale bars shown on the right. (**B**) Polar plot of the CMD of the HD tuning curve (dots). A red vector originating from the center depicts a mean vector with a CMD and MVL as a direction and magnitude, respectively. Solid lines represent the 95% confidence interval for the mean direction. The circle radius indicates MVL = 1.0. (**C**) Polar plots of firing rate as a function of HD (red) and behavioral HD (gray), from examples of five HD cells, are shown. Black vector originating from the center depict the mean vectors with CMD and MVL as a direction and magnitude, respectively.

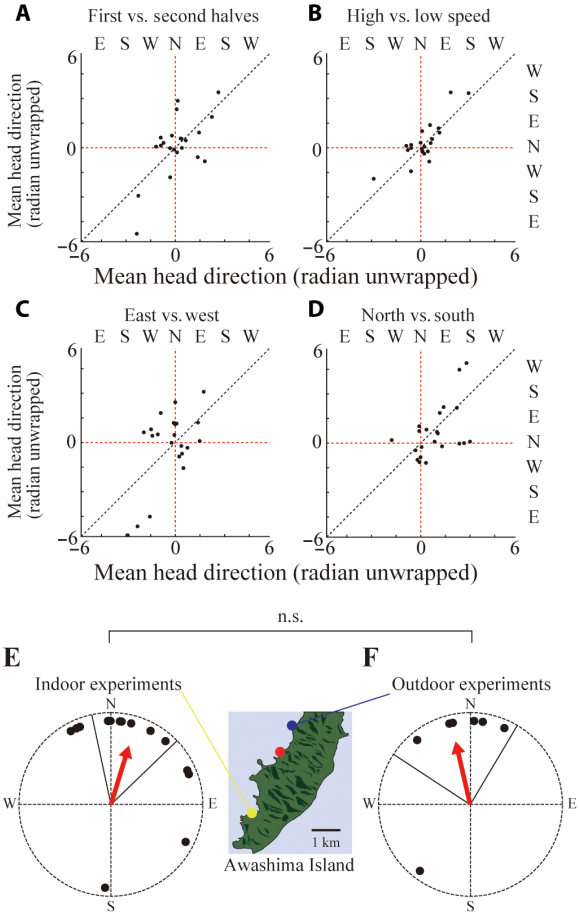

Fig. 3. North preference is stable and invariant to geolocation. (**A** to **D**) Scatter plots of the preferred direction of HD cells between the first and second halves of the session, (A) fast and slow walking speeds, (B) east and west portions of the arena, and (C) north and south portions of the arena. (D) Red dotted lines indicate the north orientation. Black dotted lines depict the identity lines. (**E** and **F**) Polar plot of the CMD of the HD tuning curve (dots) in indoor (E) or outdoor (F) experiments. Red vectors originating from the center depict mean vectors with CMD and MVL as a direction and magnitude, respectively. Solid lines represent the 95% confidence interval for the mean direction. The circle radius indicates MVL = 1.0. N, E, S, and W indicate geomagnetic north, east, south, and west, respectively. Indoor and outdoor experiments were conducted at the yellow and blue circles on the map of Awashima Island, Japan, respectively. Red circle indicates the location of the burrows. n.s., $P > 0.05$.

from an animal. For all four possible combinations, the preferred directions remained as north and were not significantly different (overall: CMD of 5 to 12° and MVL of 0.66 to 0.70; Rayleigh's test, $P < 0.001$; indoor experiment: CMD of 10 to 31° and MVL of 0.58 to 0.76; Rayleigh's test, $P < 0.05$; outdoor experiment: CMD of 347 to 353° and MVL of 0.71 to 0.93; Rayleigh's test, $P < 0.05$; Watson-Williams test, $P > 0.12$; fig. S12).

The HD cells identified with the moderate criterion may have a residual MVL in the HD space in response to hidden encoded variables coherently changing with HD. To corroborate the result, we further identified HD cells using more stringent criteria. Using both the 95th percentile and 0.25 MVL as a cutoff, the number of HD cells was significantly larger than expected (15 HD cells, $P < 0.0001$, one-tailed exact binomial test with an expected P_0 of 0.05). The preferred directions for the population of HD cells in the indoor and outdoor experiments remained as north and were not significantly different (indoor experiment: CMD of 9° and MVL of 0.78; Rayleigh's test, $P < 0.001$; outdoor experiment: CMD of 354° and MVL of 0.91; Rayleigh's test, $P < 0.05$; Watson-Williams test, $P > 0.53$; fig. S13, A to D). Moreover, using both the 99th percentile and 0.25 MVL as a cutoff, the number of HD cells was also significantly larger than expected (7 HD cells, $P < 0.0001$, one-tailed exact binomial test with an expected P_0 of 0.01). The preferred directions for the population of HD cells in the indoor and outdoor experiments remained as generally north (indoor experiment: CMD of 355° and MVL of 0.98; Rayleigh's test, $P < 0.01$; outdoor experiment: CMD of 352° and MVL of 0.85; Rayleigh's test, $P < 0.26$; fig. S13, E to H).

These results suggest that the north preference is not explained by geolocation or distal sensory cues. Thus, local sensory cues around the arena or unknown geolocation-invariant cues pointing to the north may be contributing factors.

Role of local cues in HD cell orientation

Last, to exclude the possibility that the change in local sensory cues influences the northward overrepresentation of HD cells, we conducted additional experiments in which chicks were subjected to experience different arenas in the following sequence: first familiar arena, probe arena with different shape, and last familiar arena with the same shape as the first familiar arena. During environmental manipulation, we investigated the effects of local cues on determining the preferred direction of HD cells. In the initial sessions, chicks

subjected to environmental manipulation in a familiar arena (large square or circle) randomly explored the open arena but exhibited a preference to stand still in later sessions, particularly in the session of arena deformation (fig. S14). Therefore, neural activity recordings with sufficient head orientation and movement samplings could be consistently collected in a few experiments throughout the entire sequence of manipulation. Consequently, we examined three manipulations of arena deformation and six manipulations of repeated exposures to the same-shaped arena.

During the first and probe sessions in arena deformation, 18 of 47 recorded cells were identified as significant HD cells with the moderate 95th percentile criterion in either session, whereas 13 cells were silent in either session. The preferred direction for the population of HD cells was mostly toward the north in both sessions (first session: CMD of 49° and MVL of 0.48; Hermans-Rasson test, $P < 0.05$; probe session: CMD of 25° and MVL of 0.52; Hermans-Rasson test, $P < 0.05$; Fig. 4A and fig. S15A). Similarly, during the first and last sessions conducted in identically shaped familiar arenas, 20 of 70 recorded cells were identified as significant HD cells with the moderate 95th percentile criterion in either session, whereas 36 cells were silent in either session. The preferred direction generally remained north between repeated exposures of the same-shaped arena (first session: CMD of 25° and MVL of 0.48; Hermans-Rasson test, $P < 0.001$; last session: CMD of 332° and MVL of 0.69; Hermans-Rasson test, $P < 0.001$; Fig. 4B and fig. S15B). Even using the CMD of the equally subsampled HD tuning curves as a preferred direction, a northward overrepresentation was observed (arena deformation: first session: CMD of 42° and MVL of 0.45; and Hermans-Rasson test, $P < 0.05$; probe session: CMD of 15° and MVL of 0.45; Hermans-Rasson test, $P < 0.05$; repeated exposure: first session: CMD of 18° and MVL of 0.47; Hermans-Rasson test, $P < 0.05$; last session: CMD of 326° and MVL of 0.70; Hermans-Rasson test, $P < 0.01$; fig. S16).

However, the number of cells consistently identified as an HD cell over the arena manipulations period was low (arena deformation: 4 of 18 HD cells; repeated exposures: 6 of 20 HD cells; fig. S17). Furthermore, the proportion decreased using a more stringent criterion with an MVL cutoff for HD at MVL > 0.25 (arena deformation: 1 of 6 HD cells; repeated exposures: 0 of 11 HD cells). Even when using the CMD of the equally subsampled HD tuning curves as a preferred direction, the number was also low (arena deformation: 6 of 20 HD cells; repeated exposures: 4 of 18 HD cells). These results suggest that the lack of stability of the HD cell population could not be easily explained by spurious HD cells.

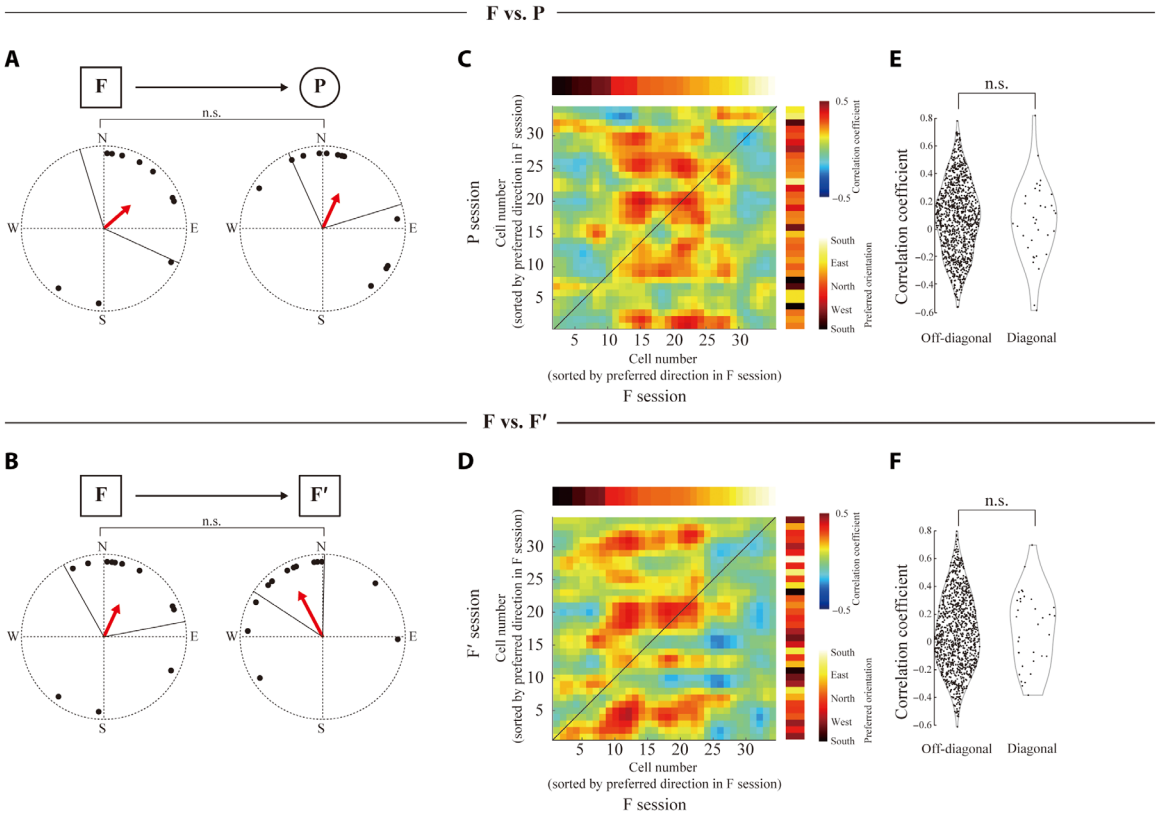

Fig. 4. North preference is stable during environmental manipulations. (**A** to **F**) Polar plots of the CMD of the HD tuning curve (dots) (A and B), cell-by-cell correlation matrices of HD tuning curves (C and D), and violin plots smoothed by a kernel density estimator of diagonal and off-diagonal values in the cell-by-cell correlation matrix (E and F) between cell pairs of the first (F) sessions exposed in a familiar arena and the probe (P) sessions with arena deformation and between cell pairs of the first (F) and last (F′) sessions exposed in a familiar arena of the same shape. The top section in (A) and (B) indicates the recording sequence. Red vectors originating from the center depict the mean vectors with CMD and MVL as a direction and magnitude, respectively. The circle radius indicates MVL = 1.0. Solid lines represent the 95% confidence interval for the mean direction. In (A) and (B), n.s.: Kuiper test, $P > 0.05$. In (C) and (D), the correlation value and preferred head orientation are color coded according to the scale bars shown on the right, respectively. The black diagonal line is drawn from the bottom-left corner to the top-right corner. In (E) and (F), n.s.: Wilcoxon rank-sum test, $P > 0.05$.

To illustrate the turnover of HD cells between sessions, we calculated cell-by-cell correlation matrices of the HD tuning curve between familiar and probe sessions and between first and last familiar sessions for cells not necessarily identified as a significant HD cell because the tuning curve of cells unidentified as an HD cell because of its low head-directionality maintained a similar HD tuning profile. As expected, HD cells with a north overrepresentation were highly correlated (Fig. 4, C and D). However, the diagonal value of the correlation matrix did not significantly differ from the off-diagonal values (Wilcoxon rank-sum test, $P > 0.60$ for both arena deformation and repeated exposure; Fig. 4, E and F). These results demonstrated that the HD cells were replaced with little overlap in response to local environmental changes; however, their population signals consistently pointed to the north.

DISCUSSION

In the present study, we recorded the electrophysiological activity of HD cells in the MP of streaked shearwater chicks before their initial migration. The overall preferred direction of the HD cell population was toward the north, like a magnetic compass. At the population level, the north preference was invariant to geolocations and distal and local sensory cues. Moreover, local environmental changes recruit HD cells with little overlap, suggesting that the HD cell signals are internally generated. Together with the fact that MR cells are present in the avian vestibular nuclei (*22*), which is a major source of the HD cell network (*12*), these results suggest that the HD sense of shearwaters at the onset of their first migration aligned in a north orientation using geolocation-invariant cues with Earth's magnetic field as a prime candidate.

The similarities in HD cell properties to other animals suggest that similar underlying neural mechanisms generate the shearwater's HD cell signals. According to the ring attractor model, a major class of computational models of HD cells (*31*), the preferred directions of HD cells in a local network always remain at a fixed angle apart, preventing all HD cells from pointing in a specific orientation in concert, as with our findings. Nevertheless, HD cells of shearwater chicks preferred to align north. Our findings raise the question of whether an HD ring attractor is conserved across animal species or whether species with migratory needs have an alternative system favoring particular cardinal directions.

According to the literature, the preferred direction of HD cells in quails and rodents rotates with a predominant cue (*10*, *14*, *32*). Although HD cells consistently identified over the environmental manipulations were scarce, we could not clarify the presence of the predominant cue anchoring the HD preference. However, as animals often do not use Earth's magnetic field when other cues are present (*23*), it is possible that HD cells of shearwater chicks are anchored by a predominant cue under certain conditions. In contrast, magnetically sensitive proteins are in the avian retina (*4*–*6*). Examination of the effect of light brightness to the northward overrepresentation of HD cells will improve our understanding of the integration pathway for the sense of direction and magnetoreception. Therefore, cue-rotation or dark-room experiments are required to unequivocally understand the difference in HD cell properties between shearwaters and mammals and the relationship between the sense of direction and magnetoreception.

The HD cells of shearwater chicks may be part of a magnetic compass that guides the first migration of juveniles to the wintering grounds in a south orientation regardless of risky mountain crossings (fig. S18) (*26*, *27*). The difference in HD cell properties between chicks and adults, and particularly whether the northward overrepresentation can be observed in HD cells of shearwater adults, will strengthen this speculation. However, the complexity of magnetoreceptor systems suggests that there are several other possibilities. For example, two different types of magnetic compass responses, each likely based on a different mechanism, exist in some birds (*5*). Other animals, such as sea turtles, have a well-developed magnetic map sense (not just a compass) that functions in navigation (*33*, *34*). A magnetic map may benefit from being oriented relative to magnetic north, and HD cells in shearwaters may be part of such a map system in birds. Furthermore, as several animal species spontaneously align their bodies north or south with the magnetic field for unknown reasons (*1*, *35*), HD cells in shearwaters may be involved in this type of behavior rather than in migration. These hypotheses will be tested using interventions of magnetic field around the birds using a magnetic coil system (*22*, *34*) in future experiments.

The magnetic compass and migratory activities of animals have been extensively studied on the basis of animal behaviors during migration, external stimuli, including geomagnetic, celestial, and olfactory cues (*7*, *19*, *29*); however, experimental studies on the relevant mechanisms acting within the brain are lacking. Our findings suggest that avian compass-like population coding can be used to gain insights into the neuronal underpinning of animal migration in natural environments (*36*) and influence the cognitive map theory (*16*) and ring attractor model of HD cells (*9*, *31*).

MATERIALS AND METHODS

Ethics statement

All procedures used in this study were approved by the Nagoya University Institutional Animal Care and Use Committee. All protocols were also approved by the Ministry of the Environment, Japan.

Animals

Ten streaked shearwater chicks (*C. leucomelas*; 1 to 2.5 months old; 450 to 760 g at electrode implantation; five males and five females) were used in this study (table S1). A few days before the experiment, the chicks were captured from their burrows on Awashima Island, Japan (38°28′N, 139°14′E). Except when recording, the shearwaters were housed individually in light-shielding cages (53 cm by 36 cm by 33 cm) and fed minced fish daily to maintain the body weight.

Surgery, electrode preparation, and recording

Under isoflurane anesthesia, a custom-made three dimensionally (3D) printed microdrive with four or eight independently movable tetrodes [12.5-μm tungsten wires with H-Formvar insulation (California Fine Wire, Grover Beach, CA, USA); without gold-plating; ~600 kilohms at a frequency of 1 kHz] was fixed to the skull above the MP of the right or left hemisphere (−2.0 mm from lambda, 1.0 to 2.0 mm lateral from midline, and 0.5 to 1.0 mm dorsal to ventral). Two anchor screws above the cerebellum were connected and served as the ground and reference point for neuronal recordings. After surgery, the tetrodes were individually lowered using the microdrive for over a week. In a single session, we recorded neuronal activity in the MP of the chicks as they walked freely in either a circular (diameter, 80 or 120 cm) or square (120 cm by 120 cm) open arena for ~10 min (Fig. 1A). The floors and the wall (30 cm high) were colored as blue.

To prevent the birds from escaping from the arenas, they were surrounded by fences (75 cm high). Before each recording session, the arena floor was cleaned thoroughly to remove odors. Wild shearwater chicks do not eat food from nonparents and can tolerate fasting for more than a week; therefore, they did not forage, even when food was scattered in the open arena. Therefore, there was no feeding during the recordings.

Extracellular signals were amplified, buffered, digitized, and continuously sampled at 31.25 or 30.0 kHz using a lightweight 16-channel or 32-channel logger (MouseLog-16B, Deuteron Technologies, Jerusalem, Israel) weighing ~6 g with a battery or a miniLogger 32 (SpikeGadgets, San Francisco, CA, USA) weighing ~7 g with a battery to record neuronal activity on a secure digital memory card. The MouseLog-16B was used in either wide-band (1 to 7000 Hz) or narrow-band (300 to 7000 Hz) mode. The miniLogger 32 was used only in wide-band (0.1 to 7500 Hz) mode. After downloading the neural signals from the SD card, spike data were digitally filtered at 800 to 7500 Hz from the wide- or narrow-band signals. Spikes were sorted using KlustaKwik (Harris Lab, UCL, London, UK) and manually verified (*37*). The unit isolation quality was quantified for each cell based on their isolation distance (ID) index [ID, 35.5 ± 4.8 (mean ± SEM); fig. S2] (*38*).

Behavioral paradigm and experimental conditions

To examine whether geolocation or distal sensory cues affect the HD preference, we recorded neural activities in the MP of shearwater chicks while they were voluntarily walking in a room ~2.5 km away from the burrows (indoor experiments) and at ~1.0 km away from the burrows (outdoor experiments). No salient visual cues around the arena consistently pointing to a specific compass orientation throughout the indoor and outdoor experiments were present. Although the fence surrounding the arena and the arena itself were the same, the compass orientation of the open arena was randomly changed daily. Furthermore, we performed neural recordings while the shearwater chicks experienced different-shaped arenas to verify the stability of the HD preference during environmental manipulations.

Shearwater chicks live in burrows on sea-facing slopes, are fed only by their parents, and do not exhibit reward-seeking behaviors; therefore, food rewards do not influence their movement. Instead, we recorded neuronal activity while the chicks voluntarily walked. These behaviors suggest that they walked in response to novelty or anxiety during recording sessions.

Indoor experiment

Indoor experiments were conducted in a room ~2.5 km away from the burrows. There were several visible cues around the arena, including ceiling lights, desks, and chairs. The ceiling lights were considered as fixed visual cues accessible to the chicks. As there were windows only on the north side of the room, the Sun's direction was not available. Several lines of evidence for HD cells in rodents suggested that the preferred direction of HD cells changes in response to a predominant cue. Thus, a quarter of the fence was shielded with a black sheet only in 4 of 15 familiar sessions as a predominant cue.

Outdoor experiment

Outdoor experiments were conducted ~1.0 km away from the burrows on a sea-facing cliff. A vehicle for the transportation and mountain slope were visible a few meters south of the arena. The chicks were in the light-shielding cage until the beginning of the experiment to prevent identifying their heading compass orientation. Although sunlight could not be controlled and was generally from the west during experiments, they faced difficulties for identifying the compass orientation from the sun's direction available for outdoor experiments.

Environmental manipulation

We conducted additional experiments in which chicks were subjected to different arenas; arenas with different shapes (square or circle) were used for this purpose. Before starting the experiments, they were acclimated to the arenas for at least 10 min. Afterward, the chicks were allowed to walk the same arena repeatedly over two sessions. In the probe session, the shape of the arena was altered. The interval for the environmental change was ~10 min. The recordings of a session in which the chicks sat still without moving their heads during the entire period were excluded.

Analyses

Walking trajectory and HD

The leading edge and fixed base of the 3D-printed NeuroLogger case mounted on the skull were tracked using DeepLabCut (Mathis Lab, Cambridge, MA, USA) (*39*) from images captured at 30 frames per second using a USB 3.0 digital video camera with a nondistorting lens mounted 1.5 m above the open arena (Fig. 1A). The walking trajectory was reconstructed by concatenating the tracked fixed base of the case. The HD was computed from the tracked leading edge and fixed base using the inverse of the tangent function.

Compass orientation

To consistently identify the geomagnetic and geographic orientation of the head of chicks, we first identified the geographic orientation at the recording site from Google Earth. Next, we estimated the geographic orientation of the left side of the captured images using the direction of a camera supported by a horizontal pole as a reference. Last, we converted the geographic orientation to the geomagnetic orientation using a magnetic declination of −8°20′ at the recording site.

HD cell analyses

HD data were sorted in bins of 1°. The directional tuning function for each cell was obtained by dividing the total number of spikes detected while the chick's head was in a specific direction bin by the total dwell time in the direction and smoothed using a gaussian filter ($\sigma = 6$ bins). The strength of directional tuning was estimated by computing the MVL for the circular distribution of the firing rate. HD cells were defined as cells with an MVL exceeding 0.25 MVL and/or the 95th or 99th percentile of the distribution for single-cell data shuffled as described below.

Spike-timing shuffling

For each permutation trial, the entire sequence of spikes fired by a cell was time shifted along the bird's walking path by a random interval between 20 and 20 s less than the length of the trial, with the end of the trial wrapped to the beginning. A tuning function was then constructed, and an MVL was calculated. This procedure was repeated 1000 times for each cell. Last, the distribution of MVLs was computed for the entire set of permutations for each cell, and the 95th or 99th percentiles were determined.

Within-session stability

Within a single session, the stability of the preferred direction of the HD cell was assessed by calculating the Pearson product-moment correlation of the unwrapped directions or HD tuning curves between the bisected data with respect to space, time, and walking speed. Specifically, the half-time of the session, horizontal midpoint of the east-west direction, vertical midpoint of the north-south direction, and median walking speed were used as parameters.

Subsampling

To subsample the behavioral distribution to obtain equal numbers of samples in each directional bin, we first identified the smallest number of samples in the entire directional bins. Next, we randomly chose samples to obtain a number of samples equal to the smallest number and then computed subsampled neural tuning curves for HD cells in each direction bin. This procedure was repeated 100 times for each cell. The overall mean CMD of the 100 equally subsampled HD tuning curves was used as a preferred direction of each HD cell.

Cell-by-cell correlation matrix

To prepare a cell-by-cell correlation matrix of the HD tuning curves, we calculated the Pearson product-moment correlation of the HD tuning curves between the first familiar and probe sessions, as well as between the first and last familiar sessions for all recorded cells and smoothed using a gaussian filter ($\sigma = 3$ bins).

Statistical tests

Rayleigh's test was used to evaluate the uniformity of a circular distribution of HD cell firings, CMDs, or behavioral HDs. Rather than Rayleigh's test, Hermans-Rasson test was used for environmental manipulations because it outperforms Rayleigh's test in multimodal situations (*40*). Watson-Williams or Kuiper test was used for comparison when the two circular head distributions differed.

Analysis software

All analyses were performed using custom-made programs based on MATLAB functions (v9.6; MathWorks, Natick, MA, USA).

Histology

The birds were deeply anesthetized with isoflurane (Pfizer Japan, Tokyo, Japan) and transcardially perfused with phosphate-buffered saline followed by 10% phosphate-buffered formalin fixative (3.5 to 3.8% formaldehyde). The brains were removed and then cut into 40-μm coronal or sagittal slices.

To carefully consider the cytoarchitecture, the sections of one brain were stained only with cresyl violet (Nissl staining), whereas those of the remaining nine brains were divided into groups of three or four adjacent sections. Each group contained a section stained with cresyl violet (Sigma-Aldrich, St. Louis, MO, USA; C5042-10G) and two or three sections immunostained for parvalbumin (1:4000; Sigma-Aldrich, P3088), calbindin (1:500; Sigma-Aldrich, C7354), or choline acetyltransferase (1:100; Merck Millipore, Billerica, MA, USA; AB144P) (figs. S3 and S4).

To determine the precise location of the recording tetrodes in the MP, we first identified the histological landmarks (lateral ventricle or thin cell-sparse zone) visible with Nissl staining. The final locations of the tetrodes were identified from the Nissl-stained brain sections. Last, if the identified final location of the tetrode was different, then the recording location was estimated using an extrapolation based on the number of daily revolutions of the microdrives.

The Nissl stains showed that the electrode tracks were in the rostral part of the MP (Fig. 1B). We observed a gradation of parvalbumin immunoreactivity from weak in the apical region to strong in the lateral region along the rostrocaudal axis and from weak in the intermediate region to strong in the medial region along the mediolateral axis. Strong calbindin and choline acetyltransferase staining was observed in the superficial layers of the apical and lateral regions. The lateral ventricle, or thin cell-sparse zone, was used to define the deep border of the MP. Most recording sites (15 of 16) were distributed at the apical or lateral regions (figs. S1, S3, and S4), and the remaining recording site was accidentally located off-target at the apical hyperpallium on the border between the dorsal pallium and MP. The space-responsive cells of pigeons are mainly found in the ventral hippocampus, which is considered as the avian hippocampus proper (*15*, *41*), whereas the lateral and apical regions are located in the parahippocampal area.

SUPPLEMENTARY MATERIALS

Supplementary material for this article is available at https://science.org/doi/10.1126/sciadv.abl6848

View/request a protocol for this paper from *Bio-protocol*.

REFERENCES AND NOTES

1. S. Begall, J. Červený, J. Neef, O. Vojtěch, H. Burda, Magnetic alignment in grazing and resting cattle and deer. *Proc. Natl. Acad. Sci. U.S.A.* **105**, 13451–13455 (2008).
2. K. Thorup, I. A. Bisson, M. S. Bowlin, R. A. Holland, J. C. Wingfield, M. Ramenofsky, M. Wikelski, Evidence for a navigational map stretching across the continental U.S. in a migratory songbird. *Proc. Natl. Acad. Sci. U.S.A.* **104**, 18115–18119 (2007).
3. F. Sergio, A. Tanferna, R. De Stephanis, L. L. Jiménez, J. Blas, G. Tavecchia, D. Preatoni, F. Hiraldo, Individual improvements and selective mortality shape lifelong migratory performance. *Nature* **515**, 410–413 (2014).
4. J. Xu, L. E. Jarocha, T. Zollitsch, M. Konowalczyk, K. B. Henbest, S. Richert, M. J. Golesworthy, J. Schmidt, V. Déjean, D. J. C. Sowood, M. Bassetto, J. Luo, J. R. Walton, J. Fleming, Y. Wei, T. L. Pitcher, G. Moise, M. Herrmann, H. Yin, H. Wu, R. Bartölke, S. J. Käsehagen, S. Horst, G. Dautaj, P. D. F. Murton, A. S. Gehrckens, Y. Chelliah, J. S. Takahashi, K.-W. Koch, S. Weber, I. A. Solov'yov, C. Xie, S. R. Mackenzie, C. R. Timmel, H. Mouritsen, P. J. Hore, Magnetic sensitivity of cryptochrome 4 from a migratory songbird. *Nature* **594**, 535–540 (2021).
5. R. Wiltschko, T. Ritz, K. Stapput, P. Thalau, W. Wiltschko, Two different types of light-dependent responses to magnetic fields in birds. *Curr. Biol.* **15**, 1518–1523 (2005).
6. R. Wiltschko, W. Wiltschko, Magnetoreception in birds. *J. R. Soc. Interface* **16**, 20190295 (2019).
7. H. Mouritsen, Long-distance navigation and magnetoreception in migratory animals. *Nature* **558**, 50–59 (2018).
8. E. Vinepinsky, L. Cohen, S. Perchik, O. Ben-Shahar, O. Donchin, R. Segev, Representation of edges, head direction, and swimming kinematics in the brain of freely-navigating fish. *Sci. Rep.* **10**, 14762 (2020).
9. J. D. Seelig, V. Jayaraman, Neural dynamics for landmark orientation and angular path integration. *Nature* **521**, 186–191 (2015).
10. J. S. Taube, R. U. Muller, J. B. Ranck, Head-direction cells recorded from the postsubiculum in freely moving rats. I. Description and quantitative analysis. *J. Neurosci.* **10**, 420–435 (1990).
11. A. Finkelstein, D. Derdikman, A. Rubin, J. N. Foerster, L. Las, N. Ulanovsky, Three-dimensional head-direction coding in the bat brain. *Nature* **517**, 159–164 (2015).
12. R. M. Yoder, J. S. Taube, The vestibular contribution to the head direction signal and navigation. *Front. Integr. Neurosci.* **8**, 32 (2014).
13. R. W. Stackman, J. S. Taube, Firing properties of head direction cells in the rat anterior thalamic nucleus: Dependence on vestibular input. *J. Neurosci.* **17**, 4349–4358 (1997).
14. E. Ben-Yishay, K. Krivoruchko, S. Ron, N. Ulanovsky, D. Derdikman, Y. Gutfreund, Directional tuning in the hippocampal formation of birds. *Curr. Biol.* **31**, 2592–2602.e4 (2021).
15. C. Herold, V. J. Coppola, V. P. Bingman, The maturation of research into the avian hippocampal formation: Recent discoveries from one of the nature's foremost navigators. *Hippocampus* **25**, 1193–1211 (2015).
16. E. C. Tolman, Cognitive maps in rats and men. *Psychol. Rev.* **55**, 189–208 (1948).
17. J. O'Keefe, L. Nadel, *The Hippocampus as a Cognitive Map* (Oxford Univ. Press, 1978).
18. T. Hafting, M. Fyhn, S. Molden, M. Moser, E. I. Moser, Microstructure of a spatial map in the entorhinal cortex. *Nature* **436**, 801–806 (2005).
19. S. Johnsen, K. J. Lohmann, The physics and neurobiology of magnetoreception. *Nat. Rev. Neurosci.* **6**, 703–712 (2005).
20. L. Q. Wu, J. D. Dickman, Magnetoreception in an avian brain in part mediated by inner ear lagena. *Curr. Biol.* **21**, 418–423 (2011).
21. N. Keary, H. J. Bischof, Activation changes in zebra finch (*Taeniopygia guttata*) brain areas evoked by alterations of the earth magnetic field. *PLOS ONE* **7**, e38697 (2012).
22. L. Q. Wu, J. D. Dickman, Neural correlates of a magnetic sense. *Science* **336**, 1054–1057 (2012).
23. S. Johnsen, K. J. Lohmann, E. J. Warrant, Animal navigation: A noisy magnetic sense? *J. Exp. Biol.* **223**, jeb164921 (2020).
24. V. L. Tryon, E. U. Kim, T. J. Zafar, A. M. Unruh, S. R. Staley, J. L. Calton, Magnetic field polarity fails to influence the directional signal carried by the head direction cell network and the behavior of rats in a task requiring magnetic field orientation. *Behav. Neurosci.* **126**, 835–844 (2012).

25. W. Wiltschko, R. Wiltschko, Global navigation in migratory birds: Tracks, strategies, and interactions between mechanisms. *Curr. Opin. Neurobiol.* **22**, 328–335 (2012).
26. K. Yoda, T. Yamamoto, H. Suzuki, S. Matsumoto, M. Müller, M. Yamamoto, Compass orientation drives naïve pelagic seabirds to cross mountain ranges. *Curr. Biol.* **27**, R1152–R1153 (2017).
27. K. Yoda, M. Okumura, H. Suzuki, S. Matsumoto, S. Koyama, M. Yamamoto, Annual variations in the migration routes and survival of pelagic seabirds over mountain ranges. *Ecology* **102**, e03297 (2021).
28. A. Rubin, M. M. Yartsev, N. Ulanovsky, Encoding of head direction by hippocampal place cells in bats. *J. Neurosci.* **34**, 1067–1080 (2014).
29. H. Mouritsen, D. Heyers, O. Güntürkün, The neural basis of long-distance navigation in birds. *Annu. Rev. Physiol.* **78**, 133–154 (2016).
30. S. Takahashi, T. Hombe, R. Takahashi, K. Ide, S. Okamoto, K. Yoda, T. Kitagawa, Y. Makiguchi, Wireless logging of extracellular neuronal activity in the telencephalon of free-swimming salmonids. *Anim. Biotelemetry.* **9**, 9 (2021).
31. K. Zhang, Representation of spatial orientation by the intrinsic dynamics of the head-direction cell ensemble: A theory. *J. Neurosci.* **16**, 2112–2126 (1996).
32. P. A. Dudchenko, J. P. Goodridge, J. S. Taube, The effects of disorientation on visual landmark control of head direction cell orientation. *Exp. Brain Res.* **115**, 375–380 (1997).
33. K. J. Lohmann, C. M. F. Lohmann, B. el Jundi, A. Kelber, B. Webb, There and back again: Natal homing by magnetic navigation in sea turtles and salmon. *J. Exp. Biol.* **222**, jeb184077 (2019).
34. K. J. Lohmann, C. M. F. Lohmann, L. M. Ehrhart, D. A. Bagley, T. Swing, Geomagnetic map used in sea-turtle navigation. *Nature* **428**, 909–910 (2004).
35. S. Begall, E. P. Malkemper, J. Červený, P. Němec, H. Burda, Magnetic alignment in mammals and other animals. *Mamm. Biol.* **78**, 10–20 (2013).
36. G. Lahvis, Animal welfare: Make animal models more meaningful. *Nature* **543**, 623 (2017).
37. K. D. Harris, D. A. Henze, J. Csicsvari, H. Hirase, G. Buzsaki, Accuracy of tetrode spike separation as determined by simultaneous intracellular and extracellular measurements. *J. Neurophysiol.* **84**, 401–414 (2000).
38. K. D. Harris, H. Hirase, X. Leinekugel, D. A. Henze, G. Buzsaki, G. Buzsáki, Temporal interaction between single spikes and complex spike bursts in hippocampal pyramidal cells. *Neuron* **32**, 141–149 (2001).
39. A. Mathis, P. Mamidanna, K. M. Cury, T. Abe, V. N. Murthy, M. W. Mathis, M. Bethge, DeepLabCut: Markerless pose estimation of user-defined body parts with deep learning. *Nat. Neurosci.* **21**, 1281–1289 (2018).
40. L. Landler, G. D. Ruxton, E. P. Malkemper, The Hermans-Rasson test as a powerful alternative to the Rayleigh test for circular statistics in biology. *BMC Ecol.* **19**, 30 (2019).
41. G. E. Hough, V. P. Bingman, Spatial response properties of homing pigeon hippocampal neurons: Correlations with goal locations, movement between goals, and environmental context in a radial-arm arena. *J. Comp. Physiol. A Neuroethol. Sens. Neural. Behav. Physiol.* **190**, 1047–1062 (2004).

Acknowledgments

Funding: This work was supported by Japanese Society for the Promotion of Science Kakenhi grants 16H06543, 19H01131, and 21H05296 for S.T., and 16H06541 and 21H05294 for K.Y.

Author contributions: Conceptualization: S.T. and K.Y. Methodology: S.T., T.H., and K.I. Software: S.T. Validation: S.T., T.H., and K.I. Formal analysis: S.T. and K.I. Investigation: T.H., K.I., S.T., and S.M. Resources: T.H., K.Y., and S.M. Data curation: S.T., T.H., and K.I. Writing–original draft: ST. Writing–review and editing: S.T. and KY. Visualization: K.I. and S.T. Project administration: S.T. and K.Y. Funding acquisition: S.T. and K.Y. **Competing interests:** The authors declared that they have no competing interests. **Data and materials availability:** All data needed to evaluate the conclusions in the paper are present in the paper and/or the Supplementary Materials. The datasets and custom-written MATLAB codes used for data analysis are available from the Zenodo repository (DOI: 10.5281/zenodo.5576843).

Submitted 29 July 2021
Accepted 13 December 2021
Published 4 February 2022
10.1126/sciadv.abl6848